Effect of CNT Addition on the Characteristics of Cu-Ni/CNT Nanocomposite

P. Bakhshaei, A. Ataie*, H. Abdizadeh

School of Metallurgy and Materials Engineering, College of Engineering, University of Tehran, Tehran, Iran

Corresponding author:
E-mail address:
aataie@ut.ac.ir
Phone: 98 912 1936361
Fax: +98 21 88006076

Abstract

In this study, Cu_{50}-Ni_{50} alloy were synthesized by mechanical alloying. The alloy was then reinforced by dispersion of multiwalled carbon nanotubes using a planetary high energy ball mill. X-ray diffraction, scanning electron microscopy and vibrating sample magnetometer were used to evaluate the effects of CNT addition on the characteristics of the nanocomposites. XRD results of Cu-Ni sample showed that, the homogeneous Cu_{50}-Ni_{50} alloy with a mean crystallite size of 25 nm was formed after 10 h of milling. It was found that presence of CNTs and the stage of CNT addition can alter the phase composition, morphology and magnetic properties of the nanocomposites. Also, CNTs prevent the complete dissolution of nickel in copper and change the chemical composition of the alloy. SEM micrographs revealed that the addition of CNTs caused a significant reduction of powder particle size. More ever, the distribution of CNTs in the matrix decreases the saturation magnetization and increases the coercivity of the nanocomposites.

1. Introduction

Carbon nanotubes with remarkable mechanical and physical properties have attracted considerable attention since their discovery in 1991 [1]. Their extraordinary properties such as low density, small size, high strength, high stiffness and superior thermal and electrical conductivity, make them ideal as reinforcements in composite materials [2-4]. Significant research work in the field of CNT reinforced composites, has been carried out on polymer based matrix composites and the reason of

course related to the fact that polymer processing is easier than metal processing [5, 6]. Several fabrication routes, namely powder metallurgy [7], melt processing, thermal spraying, electrochemical routes and some novel techniques like molecular level mixing, have been used to synthesize the metal-matrix nanocomposites. One of the most important challenges in the fabrication of CNT-metal matrix nanocomposites is how to disperse CNTs uniformly in metal or alloy matrix [8, 9]. Beyond the fabrication routs, mechanical alloying has been employed extensively for uniform

dispersion of CNTs in the powder mixture and in order to achieve some mechanical bonding [7, 10, 11]. The research to date has tended to focus on mechanical properties of CNT/metal matrix nanocomposites rather than physical properties [4]. So far, there has been little discussion about nanocomposites of CNTs and magnetic materials. In recent years, there has been an increasing interest in magnetic nanoparticles. That is due to their novel properties that may be used in wide range of application [12, 13]. Binary copper-nickel alloys, exhibit important magnetic properties and are identified as potential candidates for various fields of engineering [12, 14, 15]. The present study aims to synthesize and characterize of Cu-Ni/CNT nanocomposite by mechanical alloying process. The effects of CNT addition on the phase composition, morphology, chemical composition and magnetic properties of the nanocomposite samples were systematically studied.

2. Experimental

The starting materials in this study consisted of Cu (purity of 99%) and Ni (purity of 99%) powders. The multiwalled carbon nanotubes supplied by Tehran Research Institute of Petroleum Industry with an average diameter of 10-20 nm, average length of 10 µm and purity more than 85%, used as reinforcement materials in this work (Fig. 1). The CNTs were dispersed in ethanol by ultrasonic agitation for 15 min and then dried in oven at 50°C for 24 h. Cu and Ni powders were mixed with a weight ratio of 1:1 and then milled in a high-energy planetary ball mill (PM2400) at room temperature for 20 h under the argon atmosphere. The volume of the steel vial was 150 ml. The rotation speed and the ball to powder mass ratio were 300 rpm and 20:1, respectively.
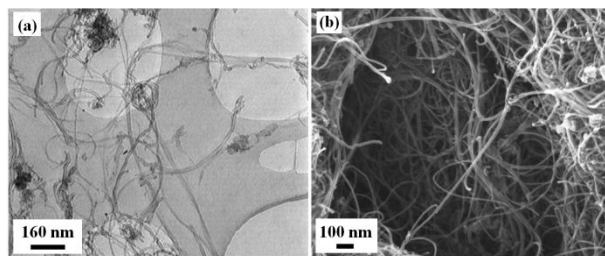

Fig. 1. (a) TEM and (b) FESEM images of carbon nanotubes.

The Cu_{50}-Ni_{50}/CNT nanocomposites were synthesised under two procedures. In the first procedure (A), mixture of Cu, Ni and 2.0 wt% CNT powders were mechanically alloyed for 15 h. In the second procedure (B), at first mixture of Cu and Ni powders were ball milled for 10 h. The alloy was then reinforced by addition of 2.0 wt% of CNTs and the mixture was subsequently ball-milled for 5 h to avoid agglomeration and structural damage of CNTs caused by milling process. Ball milling of the powder blends was carried out under the same conditions that were previously mentioned. Phases formed in the ball-milled samples were analyzed by X-ray diffraction (XRD) technique with a Philips PW-3170 diffractometer (40 kV) with Cu Kα radiation (λ = 0.154056 nm) in the 2θ range of 10-110° (step size 0.02 and time per step 0.36 s). The mean crystallite size of the samples was estimated from the broadening of the peaks for a specified phase using the Williamson-Hall plot [16]. Lattice parameters of Cu in the ball-milled samples were determined by XRD patterns. The Vegaurd's law, *i.e.,* $a_1 x + a_2(1- x) = a_0$, where a_1, a_2 and a_0 are the lattice parameter of elemental Cu, elemental Ni and Cu in binary solution, respectively, has been used to calculate the approximate dissolution of Ni in Cu after milling. The microstructures of ball-milled powders were examined by field emission scanning electron microscope (Hitachi S4160) and

SEM (Vega II Tescan) equipped with an energy dispersive spectrometer (Samx). The magnetic properties of the ball-milled samples were examined using a vibrating sample magnetometer (VSM) at the University of Kashan under the maximum magnetic field of 10 kOe.

3. Results and discussion

Fig. 2 shows the XRD patterns of Cu and Ni powders milled for various periods of times. For comparison, mixture of Cu and Ni powders without milling (NM), was also analyzed, both Cu and Ni peaks were shown in this pattern. It can be seen that on increasing the milling time, Cu and Ni peaks have approached to each other indicating the mutual dissolution of Cu and Ni. Analysis of the XRD patterns confirmed the formation of Cu_{50}-Ni_{50} alloy in a 10 h milled sample. The lattice parameter of the solid solution was found to be 3.5723 Å at this stage of milling, indicating dissolution of nickel in copper to an approximate amount of 44.9%.
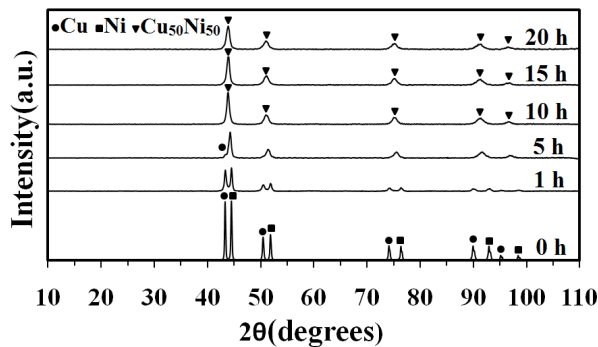
Fig. 2. XRD patterns of a mixture of Cu-Ni milled for various period of times.

Fig. 3 shows the SEM micrograph and EDS spectra of the Cu-Ni sample milled for 10 h. The detected elements in the sample were Cu, Ni, Fe and O. low concentration of O shows that oxidation has not occurred during milling process. The presence of Fe peaks is due to the

contamination from the milling equipment. The weight percents of Cu and Ni show that the alloy has a Cu/Ni ratio close to 1.
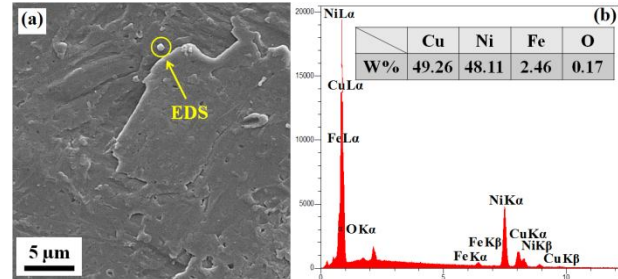
	Cu	Ni	Fe	O
W%	49.26	48.11	2.46	0.17

Fig. 3. (a) SEM image and (b) EDS spectra of the Cu-Ni milled for 10 h.

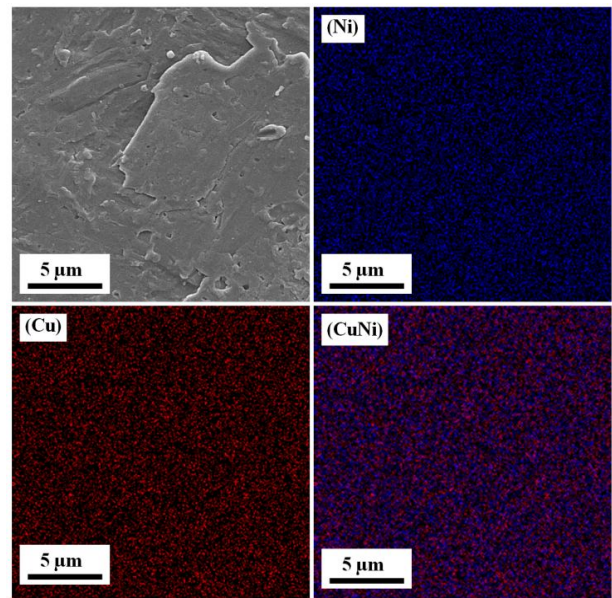Fig. 4 shows the SEM micrograph and X-ray map analysis of the 10 h milled Cu-Ni sample.

Fig. 4. SEM image with elemental analysis area scans of Cu_{50}-Ni_{50} alloy after 10 h of milling.

The elemental analysis of the sample in Fig. 4 clearly reveals that at this stage of milling, Cu and Ni have distributed uniformly in particles. It could be deduced that homogeneous Cu_{50}-Ni_{50} alloy has been produced successfully by milling process after 10 h.

The peak broadening was also occurred by increasing the milling time due to the structural refinement and increasing lattice strain. Table 1 shows the mean crystallite size of the milled samples. It is observed that the mean crystallite size is decreased by increasing the milling time. Due to the formation of Cu-Ni solid solution at early stage of milling, the crystallite size is decreased rapidly and fixed at about 17 nm.

Table 1. Mean crystallite size variation with milling time for Cu_{50}-Ni_{50} alloy

Sample	Milling time(h)	Mean crystallite size(nm)
Cu-Ni	5	50
	10	25
	15	19
	20	17

The XRD patterns of Cu-Ni-CNT powder mixture (nanocomposite A) obtained after different milling duration were shown in Fig. 5(a). The CNT peaks were not observed in the patterns due to the limitation of XRD resolution. Also, the characteristic reflections of carbide or oxide compounds were not detected. As shown in Fig. 5(b), the peaks of binary alloy were shifted towards smaller diffraction angles after 15 h of milling. It seems that the presence of CNT from the beginning of the milling process prevents the complete dissolution of nickel in copper that led to changes of the composition and magnetic properties of the nanocomposite.

This shift in diffraction angle can be explained by the following reasons. The first reason is the increase of the interplanar distances due to the presence of CNTs. The interplanar distance between (111) planes was increased from 2.05825 Å to 2.08291 Å after 15 h of milling when the CNTs was introduced in the powder mixture.
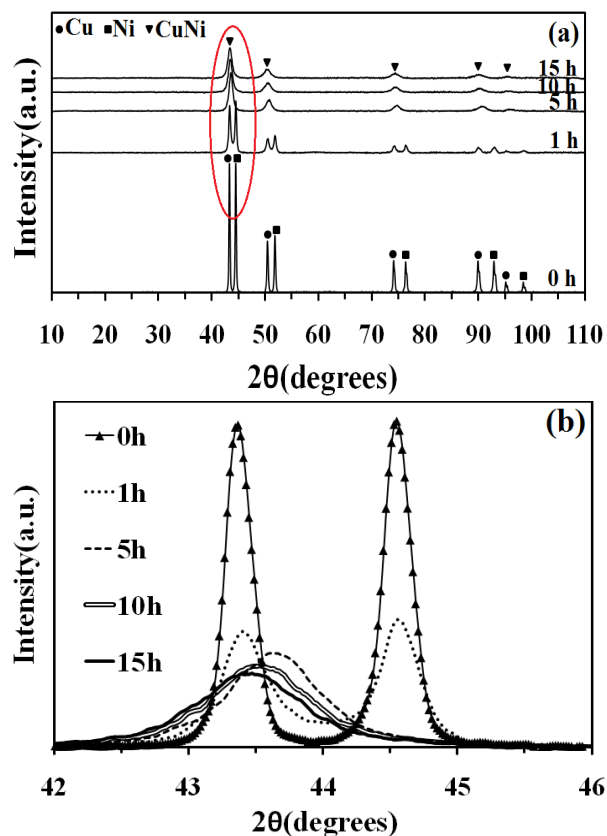

Fig. 5. (a) XRD patterns of Cu-Ni/CNT powder mixture (nanocomposite A) after different milling time and (b) magnified picture of image (a).

Another explanation could be that the CNTs act as lubricant during the milling process and decrease the milling energy imposed on the powders, hence the Cu_{50}-Ni_{50} alloy would not be formed after 15 h of milling. In addition, this shift in diffraction angle could be attributed to the topological defects, especially vacancies in carbon nanotubes [17]. Vacancies occur very frequently as native defects, they are generated in the synthesizing process. In addition by increasing the milling time, the structure of CNTs may be destroyed by deformation of powder particles during milling process and carbon atoms were pulled out from the outer walls of MWCNTs. Ni ferromagnetic metal atoms can form bonds with

defective CNTs. Hence the amount of dissolved nickel in copper was decreased.

Table 2 shows the variation of mean crystallite size with increase in milling time for the nanocomposite A. As seen, when CNTs was added to the powder mixture, a significant reduction in mean crystallite size was observed and fixed at about 8 nm. Structural refinement due to the presence of CNTs is a very important mechanism for strengthening. CNTs increase the work hardening and thermal conductivity, and act as second phases. All these leading to fine structure [4].

Table 2. Mean crystallite size variation with milling time for nanocomposite A

Sample	Milling time(h)	Mean crystallite size(nm)
Composite A	5	18
	10	12
	15	8

Fig. 6 shows the XRD patterns of nanocomposite B as compared with unreinforced alloy after 15 h of milling. It is observed that, CNTs did not affect the composition of the matrix as the second phase. Therefore, the changes in the properties of nanocomposite B as compared with $Cu_{50}-Ni_{50}$ alloy mainly attributed to the CNTs. The average crystallite size of the nanocomposite B was found to be 13 nm in a 15 h milled sample.

Fig. 7 shows the SEM micrographs of $Cu_{50}-Ni_{50}$ alloy after 10 and 15 h of milling in comparison with the nanocomposites A and B. As it can be seen, mean particle size for nanocomposite samples is smaller than that of Cu-Ni alloy. CNTs increase the work hardening and reduce the cold welding rate of the particles during the milling process and hence lead to reduce the powder particle size of the composite. As depicted in Fig.

7, more particle size reduction has happened when CNTs were introduced from the first stage of the milling process (nanocomposite A).
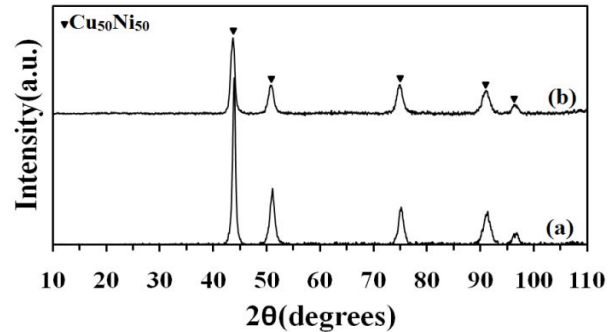

Fig. 6. XRD patterns of (a) $Cu_{50}-Ni_{50}$ alloy and (b) Cu-Ni/CNT powder mixture (nanocomposite B), after 15 h of milling.
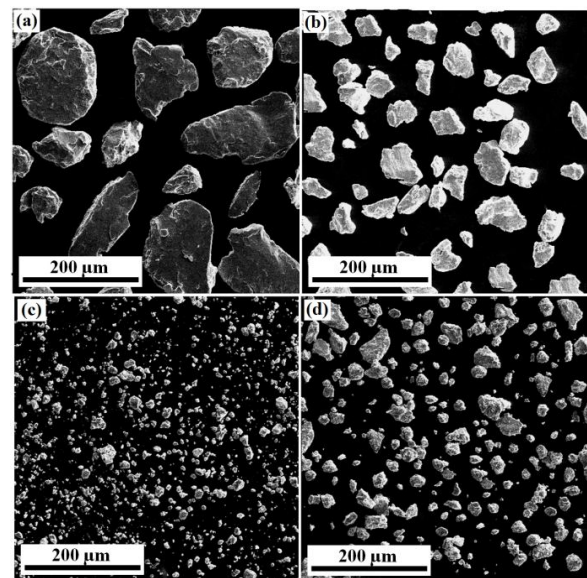

Fig. 7. SEM micrographs of (a) $Cu_{50}-Ni_{50}$ (10h), (b) $Cu_{50}-Ni_{50}$ (15h) (c) nanocomposite A and (d) nanocomposite B after 15 h of milling.

Fig. 8 (a) and (b) show the cross sectional FESEM micrographs of the nanocomposites A and B after 15 h of milling, respectively. Because of the ductility of the matrix and repeated welding that occurred during the milling process, at early stage of milling, CNTs were embedded in the matrix and do not observed on the surface of

nanocomposite particles. It can be seen from the image that the tube form of embedded CNTs have not been destroyed by milling process.
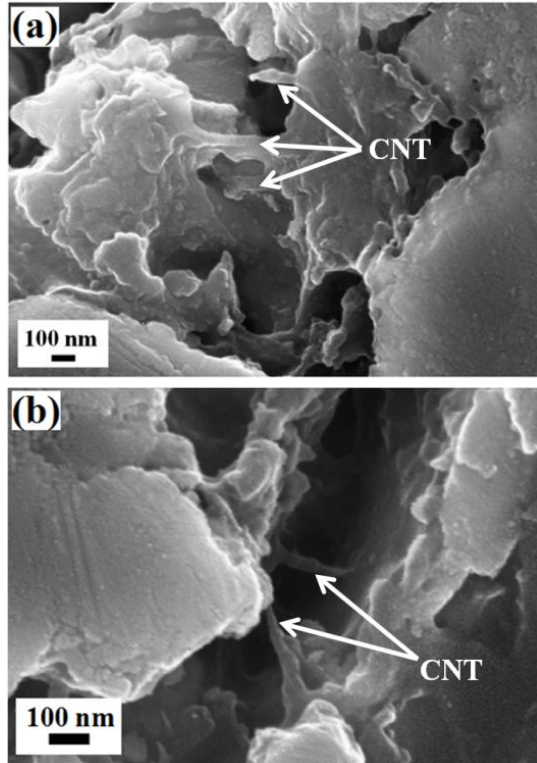

Fig. 8. FESEM micrographs of (a) nanocomposite A and (b) nanocomposite B after 15 h of milling.

Fig. 9 shows hysteresis loops of the Cu_{50}-Ni_{50} alloy, nanocomposite A and nanocomposite B. As can clearly be seen from the magnetic hysteresis loops, all of the prepared samples exhibit typical soft ferromagnetic nature. The results show that the obtained nanocomposites exhibited reduced saturation magnetization (M_s) and enhanced coercivity (H_c) as compared with unreinforced alloy. Relatively high value of coercivity in nanocomposite samples is related to their smaller particle size due to the presence of CNTs. The coercivity of the nanocomposite A with smaller particle size is higher than that of the nanocomposite B. in addition CNTs as a reinforcment phase with an anistropic shapes, led

to increase of the internal strain values and can change the magnetization mechanism of the composites. The movement of domain walls is blocked by the embedded CNTs, resulting in the change of H_c. The decreased M_s value could be related to the week magnetic properties of CNTs in the nanocomposites. This also may be due to the intraction of Ni atoms and vacancy points on the CNTs.
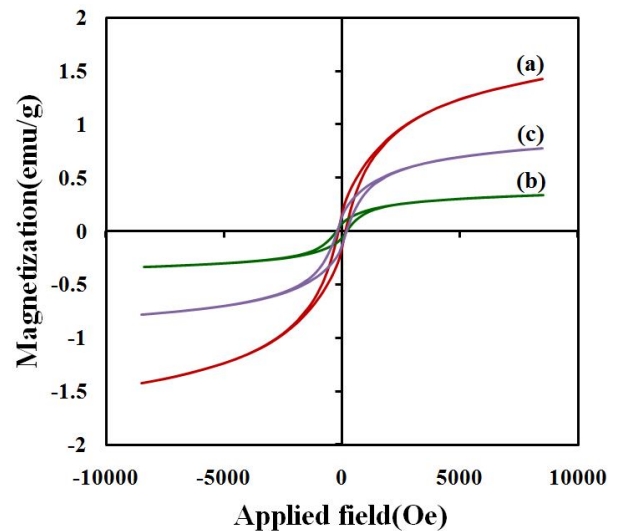

Fig. 9. Hysteresis loops of (a) Cu-Ni alloy, (b) composite A and (c) composite B.

The magnetic properties of the samples are summarized in Table 3.

Table 3. Values of coercivity and saturation magnetization of the samples

Sample	Coercivity (Oe)	Saturation Magnetization (emu/g)
Cu-Ni	150	1.4
Composite A	225	0.3
Composite B	200	0.8

4. Conclusion

In this study, the effects of CNT addition on the characteristics of Cu-Ni/CNT nanocomposite were systematically investigated. The obtained results listed as follows:

● Homogeneous Cu_{50}-Ni_{50} alloy with a mean crystallite size of about 25 nm was formed after 10 h of milling.

● Presence of CNTs and the stage of CNT addition can change the composition, microstructure and magnetic properties of the nanocomposites.

● Presence of CNTs from the beginning of the milling process prevents the complete dissolution of nickel in copper that led to changes of the composition and magnetic properties of the nanocomposite. While, after formation of Cu_{50}-Ni_{50} alloy, addition of CNTs as reinforcement phase did not affect the composition of the matrix and the changes in the properties of the nanocomposite mainly attributed to the presence of CNTs.

● Mean particle size of Cu_{50}-Ni_{50}/CNT nanocomposites significantly decreased with addition of CNTs.

● Saturation magnetization of the nanocomposites has decreased and coercivity increased as compared with the Cu_{50}-Ni_{50} alloy due to the presence of CNTs.

Acknowledgment

References

[1] S. Iijima, Nature. 354 (1991) 56-58.

[2] A. M. K. Esawi, M. M. Farag, Materials & Design. 28 (2007) 2349-2401.

[3] P. J. F. Harris, International Materials Reviews. 49 (1) (2004) 31-43.

[4] S. R. Bakshi, D. lahiri, A. Agarwal, International Materials Reviews. 55 (1) (2010) 41-64.

[5] A. Bhat, V. K. Balla, S. Bysakh, D. Basu, S. Bose, A. Bandyopadhyay, Materials Science and Engineering: A. 528 (2011) 6727-6732.

[6] E. Neubauer, M. Kitzmantel, M. Hulman, P. Angerer, Composites Science and Technology. 70 (2010) 2228-2236.

[7] R. Pérez-Bustamante, F. Pérez-Bustamante, I. Estrada-Guel, C. R. Santillán-Rodríguez, J. A. Matutes-Aquino, J. M. Herrera-Ramírez, M. Miki-Yoshida, R. Martínez-Sánchez, Powder Technology. 212 (2011) 390-396.

[8] S. R. Bakshi, R. G. Batista, A. Agarwal, Composites: Part A. 40 (2009) 1311-1318.

[9] A. H. Javadi, Sh. Mirdamadi, M. A. Faghisani, S. Shakhesi, World Academy of Science, Engineering and Technology. 59 (2011) 16-22.

[10] R. George, K. T. Kashyap, R. Rahul, S. Yamdagni, Scripta Materialia. 53 (2005) 1159-1163.

[11] H. Bahmanpour, K. M. Youssef, R. O. Scattergood, C. C. Koch, Journal of Materials Science. 46 (2011) 6316-6322.

[12] B. N. Mondal, A. Basumallick, P. P. Chattopadhyay, Materials Chemistry and Physics. 110 (2008) 490-493.

[13] Zh. Zheng, B. Xu, L. Huang, L. He, X. Ni, Solid State Sciences. 10 (2008) 316-320.

[14] I. Ban, J. Stergar, M. Drofenik, G. Ferk, D. Makovec, Journal of Magnetism and Magnetic Materials. 323 (2011) 2254-2258.

[15] E. H. Williams, Physical Review. 38 (1931) 828-832.

[16] G. K. Williamson, W. H. Hall, Acta Metall. 1 (1953) 22-31.

[17] H. L. Zhuang, G. P. Zheng, A. K. Soh, Computational Materials Science. 43 (2008) 823-828.